Applied Physics Express **9**, 032401 (2016)
http://doi.org/**10.7567/APEX.9.032401**

High-sensitivity pesticide detection using particle-enhanced resonant Raman scattering

Bikas Ranjan, Yuika Saito, and Prabhat Verma*

Department of Applied Physics, Osaka University, Suita, Osaka 565-0871, Japan

*E-mail: verma@ap.eng.osaka-u.ac.jp

Received January 5, 2016; accepted January 12, 2016; published online January 27, 2016

The use of pesticides in agriculture has raised concerns, as even a small residual of pesticide on food can be harmful. It is therefore of great importance to develop a robust technique to detect tiny amounts of pesticides. Although Raman spectroscopy is frequently used for chemical identification, it is not suitable for extremely low molecular concentrations. We propose a technique called particle-enhanced resonant Raman spectroscopy to detect extremely low concentrations of pesticides, where gold nanoparticles of desired plasmonic resonance are synthesized to match the resonance in Raman scattering. We successfully demonstrated the detection of extremely low amounts of pesticides on oranges.

In order to protect agricultural food items, such as fruits and vegetables, from pests and insects, contemporary agriculture relies heavily on pesticides.[1] Increased use of pesticides may result in high yield and good quality of agricultural products, but also has harmful effects on human health as well as on the environment and other living creatures. Recently, people try to avoid such chemically grown food and are turning to so-called organic food, and as a consequence, some producers try to hide the use of pesticides in the agricultural process. Thus, it is a matter of great concern to identify the existence of pesticides and other harmful chemicals on agricultural products.[2] Indeed, researchers have directed attention to this issue and one can find several techniques that have been reported for the detection of pesticides, such as high-performance liquid chromatography,[3] gas chromatography,[4] gas chromatography mass spectroscopy,[5] capillary electrophoresis,[6] and the enzyme-linked immunity saturation technique.[7] However, these detection techniques are not very practical, as they require complicated pretreatment processes with long measurement time.

Raman spectroscopy is an accurate, nondestructive, and versatile technique for detecting vibrations originating from unique molecules and requires almost no pretreatments or sample preparation.[8] It offers "fingerprint"-like information about the molecules and biochemical constituents present in the measured sample, and has been used for decades to evaluate the safety and quality of food.[9,10] However, Raman scattering is known to be a weak phenomenon, and in its conventional form, it is only appropriate for detecting Raman signals originating from an appreciable concentration of pesticides. Raman detection becomes almost impossible at extremely low molecular concentrations. Since fruits and vegetables are well washed before they are ready to be sold in a supermarket, the concentration of pesticide molecules on the outer surface becomes very low, even though the fruit or vegetable may still contain a fair amount of pesticide inside. In such a case, since the surface concentration of pesticide molecules is low, it is hard to detect them by conventional measurement techniques, even when the total content of pesticide inside the food item may be well above the acceptable limit and may lead to long-term adverse health effects. It is therefore extremely important to find a quick, accurate, highly sensitive, specific, and easy method of detecting a wide range of pesticides at low concentrations.

One way to detect such weak Raman signals is to enhance them by several orders of magnitude by means of plasmonic techniques. This can be accomplished by, for example, surface-enhanced Raman spectroscopy (SERS),[11,12] or tip-enhanced Raman spectroscopy (TERS).[13] In SERS, the Raman signal is enhanced by utilizing a rough metallic substrate, where hot spots are created by the nanostructured roughened metal surface. This technique has shown great potential for enhancing Raman signals from chemical samples that can be spread over a surface, such as a single molecular layer. However, for large and irregularly shaped samples, such as fruits or vegetables, this technique is not suitable. Similarly, TERS utilizes a sharp tip to locally enhance Raman signals from a nanometric volume of the sample, and hence is also unsuitable for large samples. Even though SERS and TERS are great techniques for the enhancement of Raman signals from nanosized samples or from single molecular layers, they are obviously not ideal techniques when the sample is large. One needs a technique that works on the same principles as SERS and TERS, namely, plasmonic enhancement,[14–16] but can be easily utilized to detect a small amount of chemical molecules present on the surface of a large and irregularly shaped sample. In order to solve this problem, we propose to utilize metallic nanoparticles, rather than a roughened metallic surface or a sharp metallic tip. The advantage is that metallic nanoparticles can be spread over the surface of a large sample of any shape, and it can therefore enhance Raman signals from chemical molecules present on the surface. Another advantage is that the plasmonic resonance of these nanoparticles can be easily tuned by choosing an appropriate size of these metallic particles, which is beneficial for selective enhancement. This would ensure that one can measure Raman signals from pesticides on fruits or vegetables, even when the target molecular concentration is extremely low. Enhancement by plasmonic particles in a similar manner using shell-isolated nanoparticle-enhanced Raman spectroscopy (SHINERS) has recently been suggested.[17] However, one of the main advantages of our technique over SHINERS is that we can tune the plasmonic resonance of our nanoparticles to match the resonance in Raman scattering (as discussed later), which enables our technique to detect extremely low amounts of pesticides.

We call our proposed technique particle-enhanced resonant Raman spectroscopy (PERRS). In order to provide extra enhancement for easy detection of low-concentration chem-

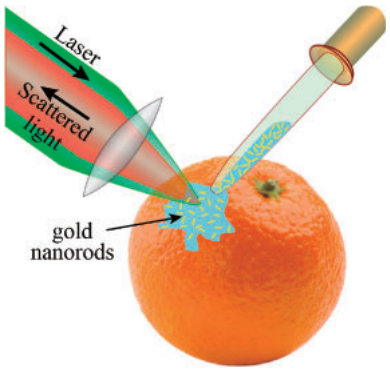

Fig. 1. Schematic illustration of PERRS experiment, where GNRs are spread over the outer surface of an orange to plasmonically enhance the resonant Raman signal from any pesticide molecules present on the surface of the orange.

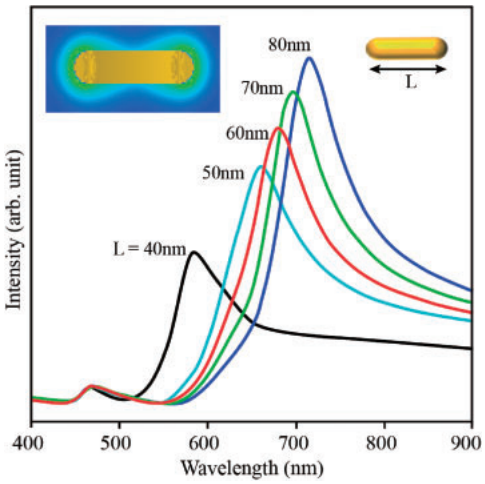

Fig. 2. Absorption spectra of GNRs with fixed diameter of 20 nm and various lengths from 40 to 80 nm, as numerically calculated using 3D-FDTD method. The left inset shows the locally enhanced electromagnetic near field for the laser excitation wavelength of 695 nm for an isolated GNR of length 70 nm.

icals, this technique also includes the resonant Raman effect. The resonance effect in Raman scattering takes place when the incident light has the same energy as the electronic energy of the sample. The resonance effect can increase the Raman cross section severalfold, and hence, enhances Raman scattering by several orders of magnitude.[18] Therefore, both resonant Raman and plasmonic enhancements together can result in a dramatic total enhancement, which is necessary for the observation of extremely low concentrations of chemical molecules. Since the resonant Raman effect takes place only at a certain wavelength of the incident light for a selected target sample, one must ensure that metallic nanoparticles also have plasmonic resonance at exactly the same wavelength, so that both enhancement mechanisms can be induced simultaneously. This means that one must design and synthesize nanoparticles such that their plasmonic resonance is tuned to the required wavelength of the resonant Raman effect for the target sample. The optimized condition for PERRS can therefore be achieved when all the plasmon resonance wavelength, excitation laser wavelength, and resonance Raman wavelength have the same value. In other words, when we select the excitation wavelength to match the resonance Raman wavelength of the sample, and design the nanoparticle to have plasmon resonance at exactly the same wavelength, PERRS will yield the best results. A strong Raman enhancement when the excitation laser wavelength matches both the Raman resonance and the plasmon resonance simultaneously was reported in the literature for SERS.[19] Figure 1 shows an illustration of the PERRS experiment, where gold nanorods (GNRs) are spread on the outer surface of an orange and the enhanced resonant Raman signal is detected from the pesticide molecules present on the fruit.

The resonance wavelength of surface plasmon polaritons (SPPs) of metallic nanoparticles is determined from the shape, size, and material.[20,21] This dependence offers flexibility to tune the SPP resonance by growing nanoparticles of the desired shape and size, so that the SPP resonance can match the resonance in Raman scattering of any target pesticide.[22] For a given pesticide, we first select an excitation wavelength to be used for PERRS measurement that falls in the resonance Raman window of the pesticide molecules and then grow the nanoparticles by selecting its size such that the SPP resonance of these nanoparticles matches the chosen excitation wavelength. In this way, both Raman scattering and plasmonic enhancement are in resonance with the excitation light, and hence, the total enhancement is boosted severalfold. Using this technique, we can detect several kinds of pesticides by changing the laser excitation to match the resonance in Raman scattering and then by tuning the SPP resonance of the nanoparticles to the same excitation wavelength.

In order to demonstrate the effectiveness of this technique, we selected two different pesticides and grew two different kinds of gold nanoparticles, namely, nanospheres and nanorods, to match both the Raman and SPP resonances. The nanoparticles were synthesized by seed-mediated growth.[23] Two commercially available pesticides, polycarbamate[24] [IUPAC name: dizinc bis(dimethyldithiocarbamate)ethylenebis(dithiocarbamate)] and benomyl[25] [IUPAC name: methyl-1-[(butylamino)carbonyl]-1*H*-benzimidazol-2-yl], which are commonly used in agriculture, were selected as target pesticides. These two pesticides show Raman resonance at two distinctly different wavelengths, thus enabling us to demonstrate tunability in our technique (see the online supplementary data at http://stacks.iop.org/APEX/9/032401/mmedia).

In order to obtain the desired plasmon resonance tunability during the synthesis of metallic nanoparticles, we first numerically simulated the scattering spectra of metallic nanoparticles by the three-dimensional finite-difference time-domain (3D-FDTD) method. The peak position of the scattering spectrum corresponds to the SPP resonance. Figure 2 shows calculated scattering spectra from GNRs with a fixed diameter of 20 nm and various lengths from 40 to 80 nm. As the lengths of the GNRs increase, the SPP resonance shows a redshift. The SPP resonance shifts from about 580 nm to about 720 nm as the lengths of the nanorods change from 40 to 80 nm. This confirms that by choosing gold as the material and nanorods as the shape, we can easily tune the SPP resonance in a broad spectral region.[20] From Fig. 2, we can estimate the required length of the GNRs for a given excitation wavelength for a particular pesticide and then synthesize the same kind of GNRs to obtain plasmonic and resonant Raman enhancements simultaneously. The left inset in Fig. 2 shows that the enhanced light field is strongly confined to the ends of a nanorod.

After numerical simulation, we proceeded to the growth of GNRs, for which we used the seed-mediated growth method, which is one of the most popular methods because of its high stability, quality, and yield.[23] This method includes two steps, namely, the seed growth process and the synthesis process. In the first step, an aqueous solution of 103 µL [24.28 mM] $HAuCl_4$ was added to a solution of 7.5 mL [0.1 M] CTAB, 1.797 mL of DI H_2O, and 600 µL of ice-cold [0.01] $NaBH_4$. The solution was vigorously stirred for 2 min and then kept in water bath at 30 °C for about 2 h, which resulted in the formation of a brownish-yellow solution. This solution contained seeds of gold with a size of approximately 3–5 nm. In the second step, various amounts of 0.01 M $AgNO_3$ were added to 10 mL of [0.1 M] CTAB, 216 µL of [24.28 mM] $HAuCl_4$, 100 µL of [0.5 M] H_2SO_4, and 80 µL of [0.1 M] ascorbic acid. The addition of ascorbic acid, a mild reducing agent, changed the growth solution from dark yellow to colorless. Finally, 24 µL of seed solution was added to the growth solutions at 30 °C and the GNRs were grown in the solution. The lengths of the GNRs were controlled by varying the silver ion concentration. When no silver ions were added, gold nanospheres (GNSs) with an average diameter of 20 nm were obtained. When silver ions were added during the synthesis process, anisotropic deposition of Ag allowed single-crystalline gold to grow with different growth rates,[23] resulting in the GNR shape. The CTAB acts as a surfactant that forms a monolayer molecular coating on the surface of gold nanoparticles. This surfactant prevents the aggregation of nanoparticles as well as chemical bonding between gold and sample molecules. As the number of silver ions increased, the length of GNRs also increased. An example of synthesized GNRs is shown in a scanning electron microscopy (SEM) image in the inset of Fig. 3, where the average diameter and average length of the synthesized GNRs are 15 and 75 nm, respectively.

The absorption spectra of synthesized GNRs shown in Fig. 3 were measured using a UV–visible spectrometer, Shimadzu UV-3600, and display two absorption peaks. The weaker absorption peak centered at 530 nm corresponds to the transverse SPP mode and it does not change its position because the diameters of all nanorods are almost the same. The stronger peak, which changes its position with the length of the nanorod, corresponds to the longitudinal SPP mode. As the concentration of silver ions was increased in the synthesis process, the nanorod size increased and the absorption spectra showed a redshift. In addition, we also synthesized GNSs without any silver ions used during the synthesis process. An absorption spectrum from the synthesized GNSs is also shown in Fig. 3; it has a prominent SPP resonance peak at about 530 nm. As estimated from the SEM images, the average diameter of the GNSs was about 20 nm. We also confirmed, from the SEM images, that the lengths of the synthesized GNRs could be changed from about 60 to 100 nm, and the absorption spectra showed that the corresponding SPP resonance shifted from about 700 to 1000 nm. One can clearly see from the absorption spectra that we can tune the SPP resonance of nanoparticles in very consistent manner, covering a wide range of the spectral region from about 500 to about 1000 nm, as shown in Fig. 3. When these synthesized nanoparticles are excited with a wavelength close to the SPP resonance, enhanced near-field light is created near the ends of the nanorods (inset in Fig. 2). If there are any

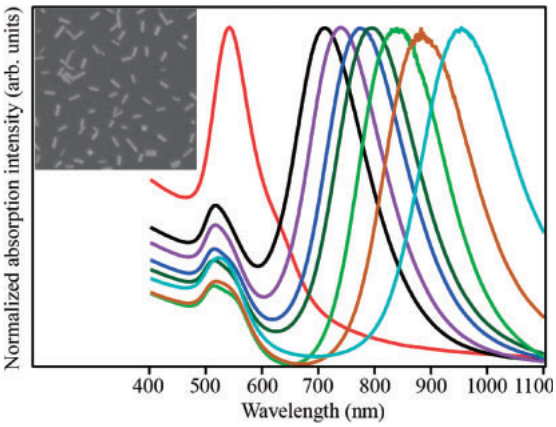

Fig. 3. Experimentally measured absorption spectra of gold nanoparticles in solution, synthesized with different silver ion concentrations. The spectrum in red, showing a peak at 530 nm, corresponds to GNSs (diameter = 20 nm), which grow in the absence of silver ions. All other spectra were measured from GNRs. One absorption peak that is fixed at about 520 nm corresponds to the transverse plasmon mode, while the other absorption peak that shifts from about 700 nm to about 1000 nm with increasing silver ion concentration corresponds to the longitudinal plasmon mode. As an example, the inset shows an SEM image of the grown GNRs with a diameter of 15 nm and a length of 75 nm, which were used in the present PERRS experiments.

pesticide molecules in this vicinity, the resonant Raman scattering from those molecules will be plasmonically enhanced to a detectable level.

Raman measurements were performed using two excitation wavelengths, $\lambda = 532$ and 785 nm, which were close to the resonances in the Raman scattering of the two target pesticides, polycarbamate and benomyl, respectively (see the online supplementary data at http://stacks.iop.org/APEX/9/032401/mmedia). The incident light was focused onto the sample through an objective lens. The same objective lens was used to collect Raman scattered light, which was directed to a spectrometer and successively detected by a CCD array detector. PERRS results are shown in Fig. 4.

In this work, we selected orange as our sample, which shows distinct Raman modes from citrus that appear at 990, 1130, and 1500 cm^{-1} [spectra (i) in Figs. 4(a) and 4(b)]. For reference, spectra (ii) in Figs. 4(a) and 4(b) show resonance Raman spectra from polycarbamate and benomyl, respectively, which exhibit many Raman modes, including a few that are strong and distinct from the citrus peaks. It should be noted that, in order to meet the resonance condition for Raman scattering from the pesticide, all spectra in Fig. 4(a) were measured with $\lambda = 532$ nm, whereas all spectra in Fig. 4(b) were measured with $\lambda = 785$ nm. After cleaning the oranges, we sprayed polycarbamate solution onto the orange in the case of Fig. 4(a) and benomyl solution onto the orange in the case of Fig. 4(b). Raman spectra exhibited strong peaks corresponding to the citrus and weak peaks corresponding to the pesticide (not shown here). We then flushed the orange several times with water to ensure that the pesticide molecules were washed out, exactly as some farmers would do to pass the chemically grown fruits or vegetables through regular food quality inspection processes. Indeed, the concentration of pesticide became so low that resonant Raman scattering showed Raman peaks corresponding only to citrus, and no pesticide peaks could be observed [spectra (iii) in Figs. 4(a)

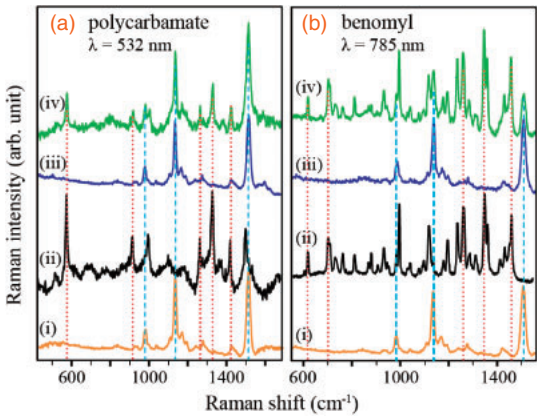

Fig. 4. Detection of extremely small amounts of (a) polycarbamate, and (b) benomyl pesticides on orange through PERRS, using excitation wavelengths $\lambda = 532$ and 785 nm, respectively. Spectra (i) represent citrus from clean oranges and spectra (ii) are from pure pesticides. Red dotted and cyan dashed vertical lines respectively indicate prominent Raman modes from pesticides and oranges. Spectra (iii) show resonant Raman scattering from oranges after a small amount of pesticide was dropped onto it and then washed off with water. These spectra show only citrus peaks, confirming that no pesticide could be detected. Spectra (iv) were taken after dropping small amounts of (a) GNSs and (b) GNRs. Raman modes from pesticides were strongly enhanced, and modes associated to both citrus and pesticides could be observed.

and 4(b)]. Next, we added GNSs (diameter = 20 nm) onto the orange that was coated with polycarbamate and GNRs (length = 75 nm) onto the orange that was coated with benomyl, keeping in mind that the GNSs and GNRs have SPP resonances near 532 and 785 nm, respectively. We expect the distribution of gold nanoparticles on the surface of orange to be similar to the image shown in the inset of Fig. 3, because nanoparticle solutions with identical concentrations were dropped and dried in both cases. However, we cannot confirm the actual distribution, because it is not possible to measure an SEM image directly form the surface of orange. Resonant Raman spectra measured after dropping the gold nanoparticles onto the orange revealed peaks corresponding to both citrus and pesticides [spectra (iv) in Figs. 4(a) and 4(b)], clearly showing that gold nanoparticles strongly enhanced the Raman signal from the pesticide molecules. For clarity, cyan dashed and red dotted vertical lines in Fig. 4 indicate some prominent peaks from orange and pesticide, respectively. It is obvious that even when the pesticide concentration was so low that conventional resonant Raman scattering was not able to detect it [spectra (iii)], the PERRS technique revealed the presence of pesticide on the fruit [spectra (iv)]. Figures 4(a) and 4(b) show that we can efficiently detect extremely low concentrations of two different pesticides that have resonance Raman scattering in two different wavelength regions. Since we do not see any Raman modes from pesticides in spectra (iii), a comparison between spectra (iii) and (iv) suggests a huge enhancement beyond calculation under the experimental limits. However, in order to get an idea of the enhancement factor, we performed a test experiment, where we used slightly higher concentrations with which we could see very weak pesticide modes in normal Raman scattering, and then compared the normal Raman intensity with the PERRS intensity. In order to calculate this enhancement factor, we considered the nanoparticle distribution to be that shown in the inset of Fig. 3, and assumed that enhanced near-field light was confined within a diameter of about 20 nm near both ends of the nanorods. The enhancement factor thus estimated was 1.7×10^6, which is similar to the value obtained from FDTD calculation, where Raman enhancement is considered to be proportional to the fourth power of field enhancement.

In conclusion, we proposed the PERRS technique to check agricultural food items for the possible use of pesticides by detecting extremely low concentrations of pesticides. We successfully demonstrated that we can tune the SPP resonance of the nanoparticle used in PERRS so that it matches the resonance in Raman scattering and hence allows us to detect extremely low concentrations of pesticide. We estimated that, in the present experiments, we successfully detected pesticides at an extremely low concentration of about 10^{-6} M. Although SERS and TERS are not suitable for large samples, such as fruits and vegetables, PERRS was found to be an extremely useful and easy technique for detecting harmful and hazardous chemicals on food items. This technique also has great potential for checking rotten or expired food, and may be extremely useful in controlling malpractice in the food business.

Acknowledgments The authors would like to thank Li Chuan Huang of National Taiwan University for help in the initial experiments and Kyoko Masui of Osaka University for support in the synthesis of nanoparticles. The authors would also like to acknowledge the financial support from the Photonics Center of Osaka University, the JSPS Asian Core Program, and a Grant-in-Aid for Scientific Research (C) 24560028. BR would like to acknowledge the financial support from MEXT.

1) Environmental Protection Agency's "Food Quality Prevention Act" (1996).
2) F. Menzinger, P. Schmitt-Kopplin, D. Freitag, and A. Kettrup, J. Chromatogr. A **891**, 45 (2000).
3) K. W. Weissmahr, C. L. Houghton, and D. L. Sedlak, Anal. Chem. **70**, 4800 (1998).
4) R. C. Perz, H. Van Lishaut, W. Schwack, and J. Agric, Food Chem. **48**, 792 (2000).
5) H. K. Lim, D. Andrenyak, P. Francom, R. L. Foltz, and R. T. Jones, Anal. Chem. **60**, 1420 (1988).
6) A. K. Malik and W. Faubel, Talanta **52**, 341 (2000).
7) K. S. Webb, P. B. Baker, N. P. Cassells, J. M. Francis, D. E. Johnston, S. L. Lancaster, P. S. Minty, G. D. Reed, and S. A. White, J. Forensic Sci. **41**, 938 (1996).
8) *Handbook of Vibrational Spectroscopy*, ed. J. M. Chalmers and P. R. Griffiths (Wiley, Chichester, U.K., 2002).
9) X. Lu, H. Al-Qadiri, M. Lin, and B. Rasco, Food Bioprocess Technol. **4**, 919 (2011).
10) P. Tanner and K. Leung, Appl. Spectrosc. **50**, 565 (1996).
11) A. M. Alak and T. Vo-Dinh, Anal. Chim. Acta **206**, 339 (1988).
12) S. Bonora, M. Di Foggia, and M. Iafisco, Chim. Ind. **90**, 98 (2008).
13) T. Umakoshi, T. Yano, Y. Saito, and P. Verma, Appl. Phys. Express **5**, 052001 (2012).
14) K. Kneipp, H. Kneipp, I. Itzkan, R. R. Dasari, and M. S. Feld, Appl. Spectrosc. **56**, 150 (2002).
15) K. A. Willets and R. P. Van Duyne, Phys. Chem. **58**, 267 (2007).
16) E. Petryayeva and U. J. Krull, Anal. Chim. Acta **706**, 8 (2011).
17) J. F. Li, Y. F. Huang, Y. Ding, Z. L. Yang, S. B. Li, X. S. Zhou, F. R. Fan, W. Zhang, Z. Y. Zhou, D. Y. Wu, B. Ren, Z. L. Wang, and Z. Q. Tian, Nature **464**, 392 (2010).
18) A. C. Albrecht, J. Chem. Phys. **34**, 1476 (1961).
19) K. Yoshida, T. Itoh, H. Tamaru, V. Biju, M. Ishikawa, and Y. Ozaki, Phys. Rev. B **81**, 115406 (2010).
20) A. Moores and F. Goettmann, New J. Chem. **30**, 1121 (2006).
21) K. Uetsuki, P. Verma, P. Nordlander, and S. Kawata, Nanoscale **4**, 5931 (2012).
22) X. Lu, M. Rycenga, S. E. Skrabalak, B. Wiley, and Y. Xia, Annu. Rev. Phys. Chem. **60**, 167 (2009).
23) A. Gole, Chem. Mater. **16**, 3633 (2004).
24) H. Kumagai, K. Nakamoto, M. Nakamura, S. Hirose, Y. Ichikawa, J. Endo, and H. Ikari, Biosci. Biotechnol. Biochem. **56**, 828 (1992).
25) F. Dane and Ö. Dalgic, Acta Biol. Hung. **56**, 119 (2005).